Oxidative Skeleton Breaking in Epoxy–Amine Networks

V. BELLENGER and J. VERDU, *Departement Matériaux, Ensam 151 Bd de l'Hôpital, 75640 Paris Cedex 13, France*

Synopsis

The photo and thermal oxidation of various epoxide–amine tridimensional polycondensates is studied by IR spectrophotometry and DSC. The network degradation results in a decrease of the glass transition temperature (T_g), which is correlated with the quantity of amide groups formed. For each system, the relative yield in skeleton breaks increases with the intensity of internal stresses. A mechanism involving the β scission of α amino alkoxy macroradicals resulting from oxidation of constrained segments of the network is proposed.

INTRODUCTION

While skeleton breaking reactions during thermal or photooxidative aging are extensively studied in the field of linear polymers, little is known in the field of tridimensional networks,[1] in which the experimental approach is considerably more difficult, essentially due to the lack of solubility. It is yet interesting, from a practical point of view, to study this phenomenon which can play an important role in surface microcracking,[2] or perhaps indirectly in hydrolytic aging.[3]

In the case of epoxy systems, a significant decrease of the glass transition temperature (T_g) has been observed during the thermal[4] or the photochemical oxidation,[5,6] essentially by means of DSC or DTA methods. However, no relevant information has been obtained on mechanisms in all cases, whereas more precise data are available for the high temperature (more than 300°C) thermal degradation.[7] For the diglycidyl ether of bisphenol A (DGEBA), crosslinked by ether bridges, Lin et al. detected by FTIR carbonyl groups as photoproducts and hypothesized that Norrish I and II processes could be responsible for the network degradation.[8]

The aim of this paper is to study the skeleton-breaking reaction in systems based on DGEBA or parent compounds and amines of the dianiline type differing by their bridge. Thin films (10–100 μm) of these polycondensates can be obtained by a previously described method.[6] Using such samples allows precise and reproducible spectrophotometric determination of some photoproducts such as carbonyl and amides, so that we can try to correlate the extent of network degradation with the initial structure and its changes during photo- and thermal degradation.

Journal of Applied Polymer Science, Vol. 30, 363–374 (1985)

CCC 0021-8995/85/010363-12$04.00

EXPERIMENTAL

Materials. Two diepoxides of the following general formula were used:

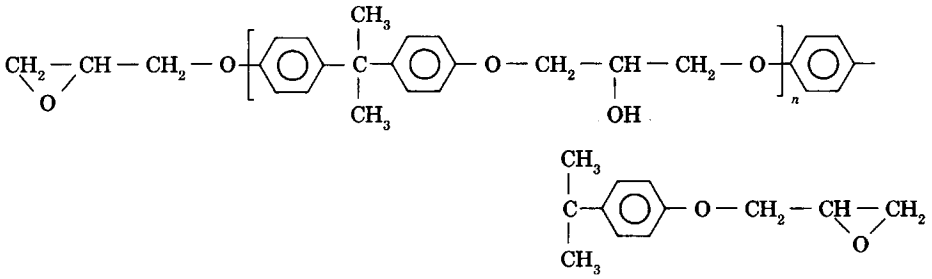

with, respectively, $\bar{n} = 0.11$ (A) and $\bar{n} = 8.8$ (B). They are crosslinked by four different diamines of the type:

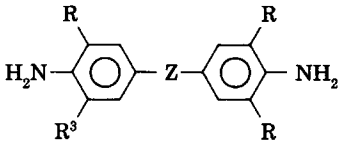

whose structural characteristics are given Table I. Two systems based on diepoxide A and the aliphatic diamines aminoethylpiperazine (AEP) and isophorone diamine (IPD), respectively, were used only in photooxidation experiments.

Samples. Films of 25–50 μm thickness were obtained by solution casting of a mixture of the two components in tetrahydrofuranne on a clean mercury surface, according to the previously published method.[6] A basic two-step thermal treatment, 1 h at 105°C followed by 1 h at 150–180°C, depending on hardener reactivity, was used to get the highest possible T_g value (the maximum value obtained whichever temperature is chosen, and which is given, for systems having epoxide and amine concentrations in stoichiometric ratio, in Table II). For systems B, the T_g value—348–351 K—is almost independent of the amine structure. In only one case, A–DDM, some samples were prepared with amine concentration differing from the stoichiometric value: Their characteristics will be given in the results section.

Exposure. For photochemical studies, we used a fluorescent lamp emitting only in the solar UV range (300–450 nm with the maximum at 365 nm). σ-Nitrobenzaldehyde[9] actinometry gave an intensity of 3.5×10^{15} photons cm^{-2} s^{-1} at sample level. The temperature was 31 ± 1°C, the films were exposed in air. At 25–50 μm thickness, the irradiation is uniform with

TABLE I
Hardener Structures

Abbreviation	Z	R
DDM	$-CH_2-$	H
DDE	$-O-$	H
DDS	$-SO_2-$	H
DDM_i	$-CH_2-$	$-CH(CH_3)_2$

depth. Thermal aging was performed in a ventilated oven, the temperatures being regulated at ±0.5°C.

Measurment. Carbonyl and amide groups were determined respectively at 1730 and 1660–1670 cm^{-1}, using the peak at 1885 cm^{-1} as internal standard with a Perkin-Elmer 580 IR Spectrophotometer. The results were expressed in absorbance units per cm thickness (cm^{-1}). T_g measurements were made with a Perkin-Elmer DSC 2, using the following conditions: weight sample, 4 ± 1 mg; temperature scanning rate, 20°C/min; sensitivity, 2 mcal s^{-1} (8.37 mJ s^{-1}). To check the reproducibility of measurements, many runs have been performed on three systems. The corresponding standard deviations are given in Table II.

RESULTS

(1) Influence of chemical structure (stoichiometric samples). An example of the infrared spectrum showing the buildup of the carbonyl and amide peaks during photooxidation is given in Figure 1.

Some IR and DSC data are summarized in Table II for photooxidation and Table III for thermal oxidation. All systems under study undergo carbonyl formation, whereas no amides appear in systems crosslinked by DDS. In photooxidation, a clear correlation between amide growth and decrease of glass transition temperature is observed (Fig. 2).

(2) Influence of cure (stoichiometric samples) on the photooxidation. For two systems undergoing the amide formation during photooxidation, A–DDM and A–DDM_i, many samples were investigated of which cure treatments were varied in order to get a range of various initial T_g values. By plotting the T_g decrease (ΔT_g) after 48 h exposure vs. initial T_g (T_{g0}), it can be shown that the network degradation increases with the initial cross-link

TABLE II
Photooxidation of Systems A and B Crosslinked by Aromatic or Aliphatic Diamines[a]

Sample	Time (h)	T_g (K)	A_{CO} (cm^{-1})	A_{amides} (cm^{-1})
A–DDM	0	438 ± 1[a]	4.6 ± 1.3[a]	0
	48	423 ± 1.5[b]	24.1 ± 4.1[b]	20.6 ± 3.5
A–DDM_i	0	415 ± 3[a]	3.5 ± 0.5[a]	0
	48	404 ± 1.5[b]	24.4 ± 1.2[b]	15.0 ± 1.2
A–DDS	0	438 ± 2.5	15.5 ± 2.4[a]	0
	48	437 ± 2[b]	27.4 ± 3.7[b]	0
A–DDE	0	433	3.2	0
	48	424	14.4	12.3
A–IPD	0	389	3.1	0
	48	390	10.1	0
A–AEP	0	442	2.9	0
	48	421	26.8	29.1
B–DDM B–DDE B–DDS	0	348 ± 3[a]	0	0
	1000	347 ± 3[b]	50 ± 10[b]	0

[a] Glass transition temperature, —C=O and amide concentrations expressed in IR absorbance units per cm thickness after 0 and 48 h of UV irradiation.

[b] Standard deviation for 10 samples.

[c] Standard deviation for six samples.

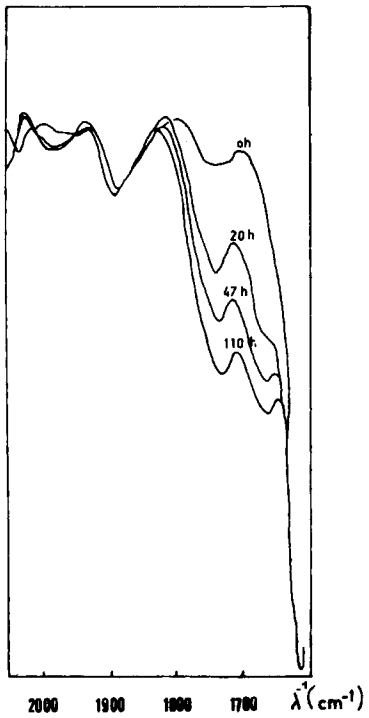

Fig. 1. Infrared spectrum of a stoichiometric sample A–DDM after 20, 47, and 110 h of UV irradiation.

density (Fig. 3), whereas no clear correlation appears, for a given system, between the rate of amide formation and T_{g0} as shown, for instance, by Table IV, which reports the results obtained for A–DDM$_i$ samples.

(3) Influence of hardener concentration (A–DDM samples) on the photooxidation. The comparison of various A–DDM samples differing by the amine concentration shows that the maximum rate of network degradation

TABLE III
Thermal Oxidation of Stoichiometric Systems A–DDM and A–DDE at various temperatures and exposture Times[a]

		A–DDM		A–DDE	
Temp (°C)	Exposure time (h)	A_{amides} (cm^{-1})	ΔT_g (°C)	A_{amides} (cm^{-1})	ΔT_g (°C)
110	566	93.8	20	52	18
120	301	103	19	93.3	27
130	198	155	16	205	38
140	79	122	16	156	30
150	40	158	18	Brittle	
165	16	62	8	166	27
180	8.5	94	13	192	25
190	4	98	11	202	17
200	2.5	143	14	219	12

[a] Amide concentration expressed in infrared absorbance units per cm thickness and corresponding decrease of the glass transition temperature.

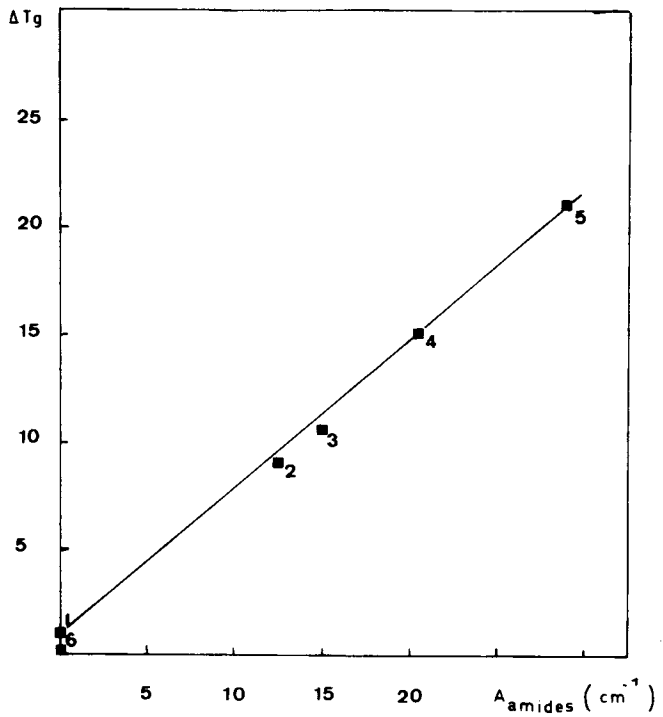

Fig. 2. Decrease of glass transition temperature vs. amide concentration expressed in absorbance units per cm thickness for stoichiometric samples: (1) A–DDS; (2) A–DDE; (3) A–DDM$_i$; (4)A–DDM; (5) A–AEP; (6) B–DDM.

is obtained for the stoichiometric value, which initially corresponds to the highest T_g value (Fig. 4). For this latter sample, an estimation of the quantum yield of chain scission has been made as follows:

$$\Phi = \frac{\Delta N_t/\Delta t}{I_0}$$

ΔN_t is the number of broken bonds at the time t, I_0 is the UV intensity 3.5 $\times$ 10^{15} photons cm^{-2} s^{-1}. From the curve of initial T_g vs. hardener concentration in Figure 3, we estimated that a ΔT_g of 15 K corresponds to a loss of 7.5% crosslinks of the stoichiometric ratio, or equivalently of 0.32 mol of broken bond per kg:

$$\frac{\Delta N_t}{\Delta t} = \frac{0.32 \times 6.02 \times 10^{23}}{10^3} \times \rho \times \mathrm{Th} \times \frac{1}{\Delta t}$$

ρ = density of sample DGEBA–DDM (g/cm^3), Th = sample thickness (cm), and Δt = irradiation time (s). We found a quantum yield of 4.5 $\times$ 10^{-4} bond broken per photon absorbed; almost four times higher than the quantum yield for amide formation in the same sample.[10]

(4) Influence of photooxidation on internal stresses. The initial thermograms of all A systems under study are characterized by the presence of

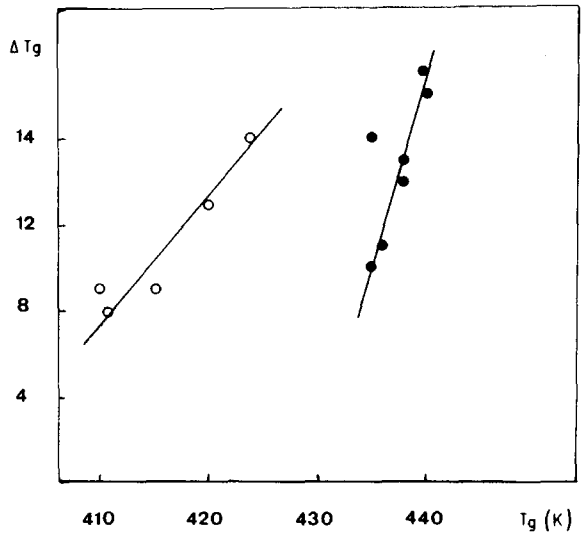

Fig. 3. Decrease of glass transition temperature (ΔT_g) after 48 h of exposure vs. initial T_g

an endothermic peak immediately following the glass transition. This peak, which disappears after an appropriate thermal treatment, for instance, a second run in the DSC apparatus (Fig. 5), can be attributed to the relaxation of internal stresses.[11] Its disappearance was also observed in the early hours of photooxidation despite the low temperature of exposure (31°C), as shown in Figure 5.

(5) Influence of temperature on network degradation. The relative efficiency of the skeleton-breaking process for a given system can be expressed by the ratio: ΔT_g/absorbance of amide peak (A_a). Indeed a rigorous analysis would be needed to compare this ratio for equivalent conversion rates of the oxidation. However, since T_g and A_a vary almost monotonously, such an approach can be used to appreciate qualitatively the sense of the variation of the "yield" in network scission with the temperature. Using the data of Table III (thermal oxidation) and Table II (photochemical oxidation), the ratio $\Delta T_g / A_a$ has been plotted vs. temperature for two systems: A–DDM and A–DDE. It is clear that, at least in the main part of the glassy state, (T < 150°C), the efficiency of the network scission process decreases with the temperature.

TABLE IV
Photooxidation of Six Samples A–DDM$_i$ with Various Initial Glass Transition Temperature[a]

Sample no.	A_{amides} after 48 h (cm^{-1})	T_g initial (K)	T_g after 48 h (K)
1	17.7	424	408
2	12.8	415	406
3	15.6	410	401
4	15.3	411	403
5	15.7	410	401
6	12.0	420	407

[a] Amide concentration expressed in infrared absorbance units per cm thickness and glass transition temperature after 48 h of UV irradiation.

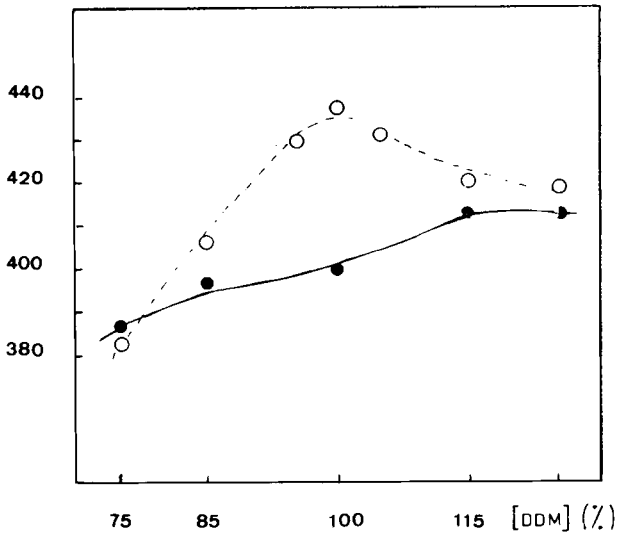

Fig. 4. T_g value versus hardener concentration expressed in % of the stoichiometric ratio before (. . .) and after (——) photooxidation.

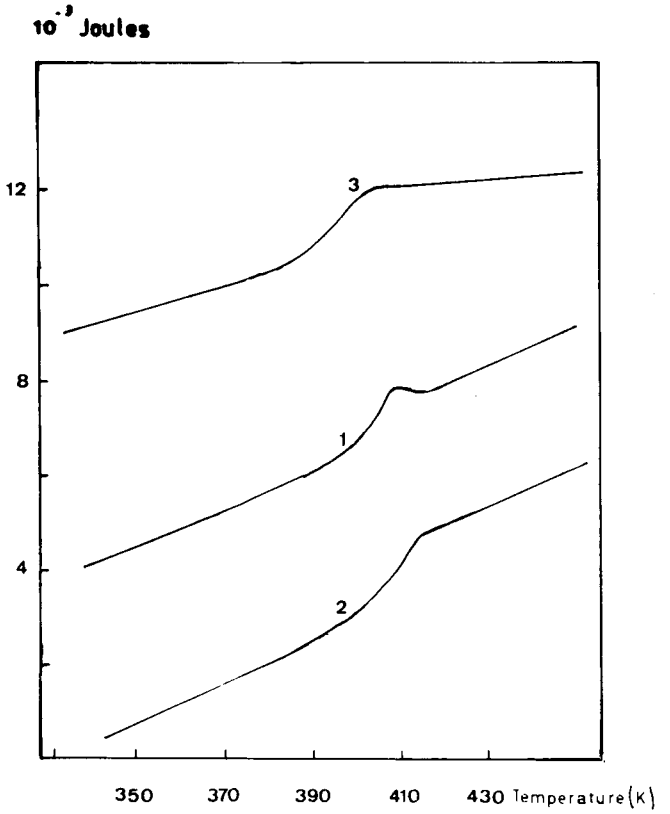

Fig. 5. Thermograms of system A–DDM$_i$: (1) first run; (2) second run; (3) first run after 96-h irradiation.

DISCUSSION

The overall mechanistic aspects of photooxidation[6,8] or thermal oxidation[12] of these systems are or will be discussed elsewhere. Concerning the skeleton breaking process, it can be concluded, from our results, that it is coupled with the amide formation. Two possible explanations can be proposed:

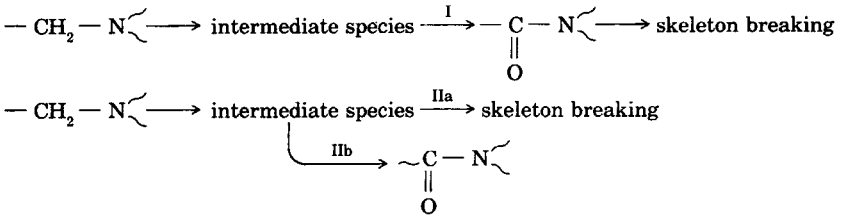

Process I seems very improbable, essentially because it implies that the "yield" in chain breaks is independent of the amine structure, and that aromatic amides are thermally unstable, which is in contradiction with all the published data on this subject and with some of our results (Table III). Process II could be compatible with the experimental data under two conditions: (i) The same intermediate species appears in both thermal and photochemical oxidation; (ii) the chemical act leading to skeleton rupture is a nonphotochemical process which does not strongly depend on amine structure, so that the rates of processes IIa and IIb vary in the same way, increasing with the amine oxidizability.

The first condition is realized if, as previously stated,[6,10] we are faced with two radical chain mechanisms, differing only by the mode of initiation:

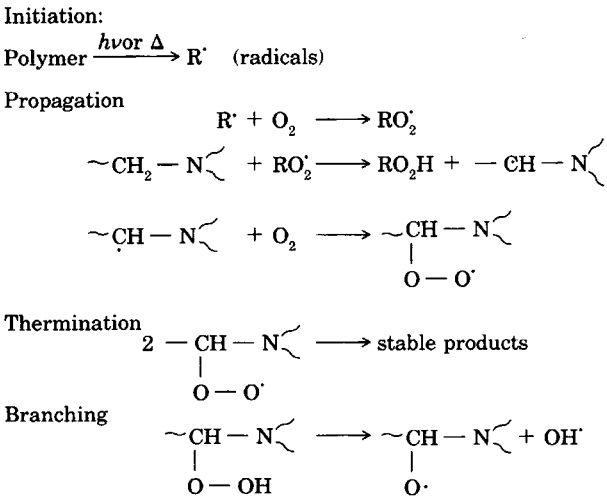

Scheme I

At least three reactions may be involved in amide formation: terminating recombination of peroxy radicals,[13] bimolecular decomposition of neighbor-

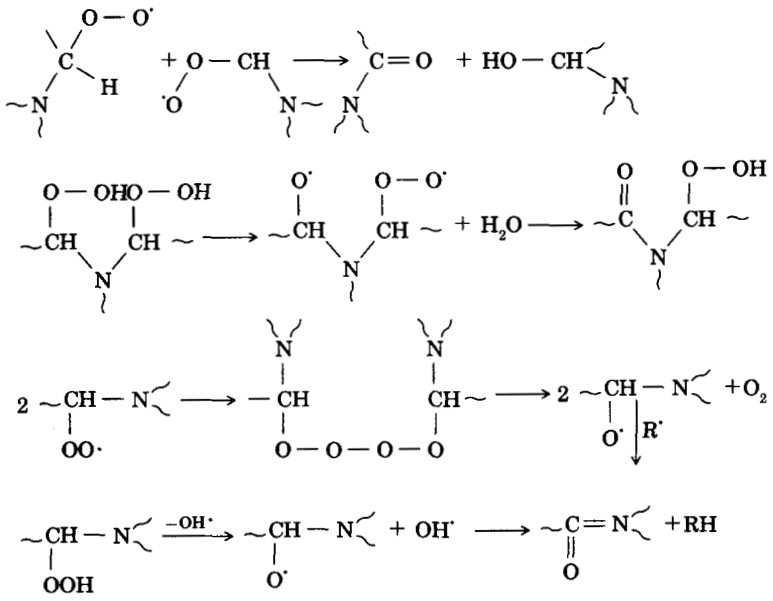

Scheme II

ing hydroperoxides,[6] or, more generally, disproportionation of alkoxy radicals resulting from hydroperoxide decomposition or nonterminating peroxy recombination (see Scheme II). Alkoxy radicals are therefore immediate precursors of amide groups. They can undergo a β scission with skeleton rupture[14]. The process IIIb seems the most probable for two reasons (see Scheme III):

(i) The carbon–carbon scission (IIIa) would lead to a substituted formamide absorbing at about 1660 cm^{-1} in IR spectrum, so that the quantum yield for amide formation would be at least equal to the quantum yield for skeleton breaks, which is not the case.

(ii) The break of the carbon-nitrogen bond (IIIb) is favored because it leads to the more stable radical, at least in the case of aromatic amines for which it is strongly stabilized by resonance. Thus, such a process could satisfy one of the two conditions needed for a correlation between amide formation and skeleton rupture in both thermal and photochemical oxidations. However, the above considerations are not sufficient to explain the variations observed in a given family of samples, for instance, A–DDM (Figs. 3 and 4) or the apparent negative temperature coefficient of the skeleton breaking

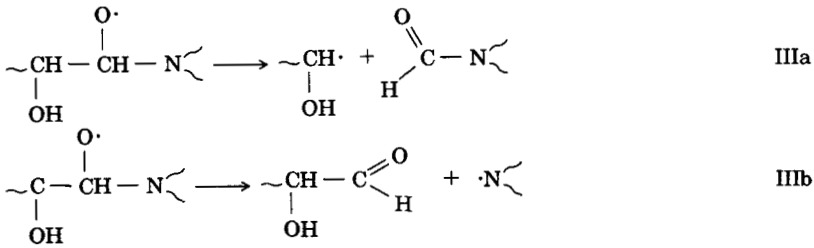

IIIa

IIIb

Scheme III

process (Fig. 5). Concerning the variation of the "yield" of network scission in a series of samples differing by the degree of polycondensation, whatever the cause of this difference, thermal history for "stoichiometric" samples (Fig. 3), or change in hardener concentration (Fig. 4), the first explanation that comes to mind can be summarized as follows: A competitive crosslinking reaction takes place in incompletely cured samples submitted to oxidation, for instance radical polymerization of end epoxide groups (in itself very improbable): However, two arguments reject this hypothesis:

(i) No crosslinking was observed in samples not completely cured which do not undergo amide formation, such as A–DDS (Table II).

(ii) The T_g decrease is lower in samples A–DDM cured with an excess of hardener than "stoichiometric" one (Fig. 4), whereas, in this case, no residual epoxide groups are present.

The following explanation seems more satisfactory: The skeleton breaking is assisted by internal stresses. It has been shown[15] that, in epoxy–amine networks, internal stresses are induced by shrinkage in the glassy state when the polymer is cooled from its cure temperature. Their intensity increases with the difference between T_g and the temperature at which they are measured. It is interesting to note that in all our experiments (Figs. 3, 4, and 6), the relative extent of network degradation (represented by ΔT_g),

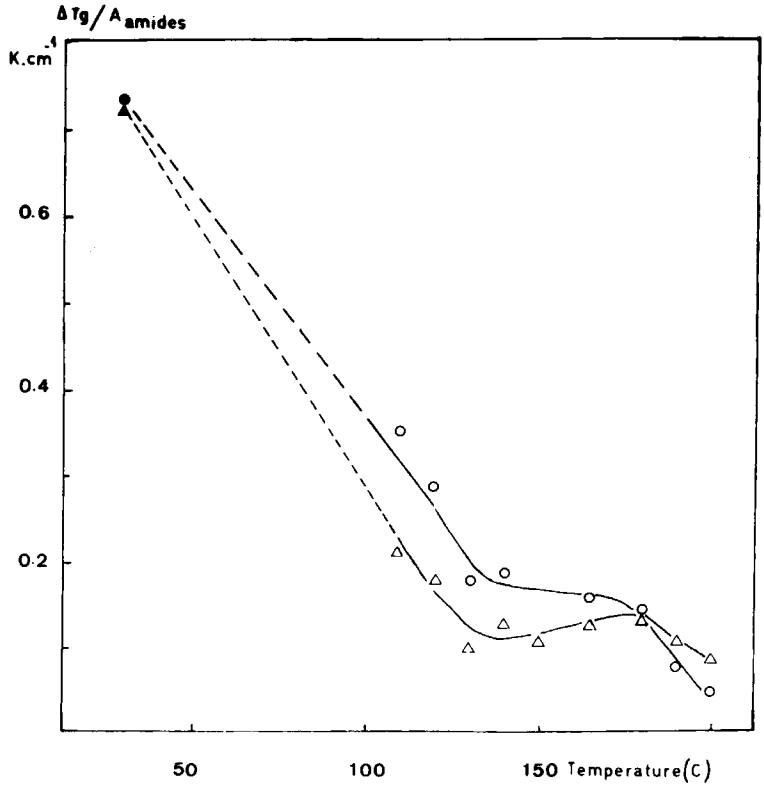

Fig. 6. ΔT_g/absorbance of amide peak vs. the temperature of the experiment for stoichiometric samples A–DDM after irradiation (▲) and after thermal oxidation (△) and A–DDE after irradiation (●) and after thermal oxidation (○).

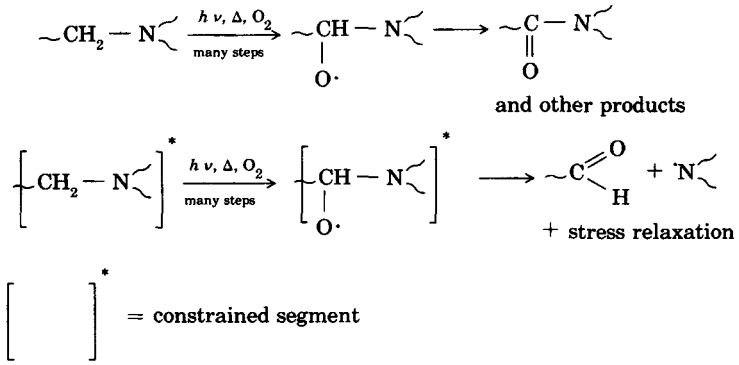

Scheme IV

increases with the difference between initial T_g and temperature of exposure at least when the latter is performed in the glassy state (Fig. 6). In other words, the "yield" in skeleton breaks is related to the intensity of internal stresses, which are influenced by the crosslink density[14] [Figs. 3 and 4 (left part)], by the plasticizing effect of residual hardener[3] [Fig. 4 (right part)], and by the temperature[15] [Fig. 6 (left part)]. If our hypothesis is valid, we can expect that backbone scissions in constrained network segments, favor the stress relaxation. This is effectively verified in the relief of internal stresses in DSC traces which disappear after 2-day photooxidation (Fig. 5), whereas no significant changes were observed, in this respect, after several months of dark storage at the same temperature.

Similar "oxidative stress relaxation" has also been observed in the case of polypropylene,[16] for which it has also been shown, on the other hand, that the rate of oxidative chain scission is enhanced in presence of mechanical stresses.[17]

Studies on model compounds of constrained molecules, such as cycloalcanes, show clearly that the deformation of valence angles increases the overall susceptibility towards oxidation,[18] but we lack data on the specific effects of stresses on skeleton breaking mechanisms.

Despite this, considering our overall results, it seems reasonable to propose the scheme IV for the network degradation in glassy state.
At higher temperature, the purely thermal β scission of alkoxy radicals and, perhaps, other mechanisms[7] can be involved in this process.

References

1. See, for instance, examples given in B. Ranby and J. F. Rabek, *Photodegradation, Photooxidation and Photostabilization of Polymers,* Interscience, New York, 1976.
2. A. Blaga and R. S. Yamasaki, *J. Mater. Sci.,* **11**, 1513 (1976).
3. R. J. Morgan and J. O'Neal, *Polym. Plast. Tech. Eng.,* **10**, 49 (1978).
4. G. T. Merral and A. C. Meeks, *J. Appl. Polym. Sci.,* **16**, 3389 (1972).
5. G. A. George, R. E. Sacher, and J. F. Sprouse, *J. Appl. Polym. Sci.,* **8**, 2241 (1977).
6. V. Bellenger, C. Bouchard, P. Claveirolle, and J. Verdu, *Polym. Photochem.,* **1**, 69 (1981).
7. J. C. Paterson-Jones, *J. Appl. Polym. Sci.,* **19**, 1539 (1975).
8. S. C. Lin, B. J. Bulkin, and E. M. Pearce, *J. Polym. Sci., Polym. Chem. Ed.,* **17**, 3121 (1979).
9. G. W. Cowell and J. M. Pitts, *J. Am. Chem. Soc.,* **90**, 1106 (1968).

10. V. Bellenger and J. Verdu, *J. Appl. Polym. Sci.*, **28**, 2599 (1983).
11. M. R. Tant and G. L. Wilkes, *Polym. Eng. Sci.*, **21**, 874 (1981).
12. V. Bellenger and J. Verdu, to appear.
13. G. A. Russel, *J. Am. Chem. Soc.*, **78**, 1047 (1956).
14. B. Ranby and J. F. Rabek, *Photodegradation, Photooxidation and Photostabilization of Polymers*, Interscience, New York, 1976, p. 100 and references cited therein.
15. M. Shimbo, M. Ochi, and Y. Shigeta, *J. Appl. Polym. Sci.*, **26**, 2265 (1981).
16. A. A. Popov, B. E. Krisyuk, N. N. Blinov, and G. E. Zaikov, *Eur. Polym. J.*, **17**, 169 (1982).
17. N. Y. Rapoport and Yu A. Shlyapnikov, *Vysokomol Soyed A*, **17**(4), 738 (1975).
18. A. A. Popov and G. E. Zaikov, *Dokl. Akad. Nauk. USSR*, **244**, 1178 (1979).

Received October 31, 1983
Accepted April 25, 1984